Flexible Boundary in Finite-Element Analysis of Pavements

RONALD S. HARICHANDRAN AND MING-SHAN YEH

The finite-element method is finding increasing use in the structural analysis of pavements. In pavement analysis, very deep finite-element meshes need to be used to satisfactorily model the infinitely deep subgrade layer. Programs require large amounts of computer memory and computational time. A scheme is developed in this paper to overcome the computational burden imposed by the requirement of a deep bottom boundary in the finite-element analysis of pavements. A flexible boundary, which accounts for displacements that occur beneath it, is used with finite elements above it. Through case studies it is shown that the method yields accurate solutions. The results are much better than those from a traditional finite-element approach requiring approximately the same amount of computational effort. The proposed method possesses significant advantages over the traditional approach, especially in nonlinear analysis.

The finite-element method is increasingly being used for the structural analysis of pavements (*1–3*). The method is especially attractive when the nonlinear behavior of the granular and cohesive materials used in pavements is to be considered in mechanistic modeling. Since the depth and width of a typical pavement are large, it is necessary when constructing the finite-element mesh to impose side and bottom boundaries at some reasonable distance from the loaded area. Along the side boundaries it is common to allow vertical displacements but not radial displacements, whereas along the bottom boundary both displacements are usually not allowed. (At interior nodes, vertical as well as radial displacements can occur.) Care must be exercised, especially with the bottom boundary, if acceptable accuracy is to be obtained in the computed displacements and stresses. When a weak subgrade is present, it is imperative that the finite-element mesh be quite deep. Use of a deep mesh, however, increases the computational effort involved, and can become prohibitive, especially for nonlinear problems where iterative or incremental solutions are required.

A technique that overcomes this drawback of the finite-element method is presented in this paper. Finite elements are used to model the soil in the vicinity of the loaded area. The side boundaries are placed, as is usual, at some distance from the loaded area (a distance of 10 to 12 times the radius of the loaded area is recommended). The bottom boundary, however, is placed at a depth below which displacements and stresses are not of interest. (In pavement design, displacements and stresses are of interest only to a depth of about 50 in.) Further, the bottom boundary is assumed to be flexible, and the half-space below the boundary is assumed to be composed of linear elastic layered material. (The boundary will usually be placed at some depth within the subgrade, in which case the half-space below the boundary will be homogeneous. The technique derived herein, however, is general and may be applied to a layered half-space.) Displacements that occur in the soil below the boundary are therefore considered in the analysis.

When dealing with nonlinear soils, the bottom boundary must be placed at a depth below which it is reasonable to neglect nonlinearities. The highly stressed, and therefore significantly nonlinear, soil in the vicinity of the loaded area can be modeled by the finite elements. This technique is computationally efficient and should yield sufficiently accurate results.

The theoretical basis for the technique discussed above is first presented, and the method is then used to analyze homogeneous and layered flexible pavement systems. Results are presented only for linear systems, and comparisons are made with the normal finite-element approach as well as exact solutions from the CHEV51 elastic layer program. The results indicate that the technique is accurate and that it is significantly better than a traditional finite-element approach requiring approximately the same amount of computational effort. The main benefits of the method are realized, however, when it is used in nonlinear analyses. The flexible boundary approach is currently being implemented in a nonlinear finite-element program being developed for the Michigan Department of Transportation. The efficiency achieved by utilizing this technique allows the program to be developed for a personal computer. Results from studies utilizing the flexible boundary with nonlinear materials will be presented at a later date.

MODELING OF FLEXIBLE BOUNDARY

Figure 1 illustrates the modeling of a pavement system. One circular wheel load is assumed, and the problem therefore reduces to an axisymmetric one. The main region of interest under the load is divided into finite elements. The finite-element mesh rests on a half-space consisting of elastic layered strata. The coupling between the finite elements and the half-space occurs at the degrees of freedom (DOF) on the bottom boundary which are shown in the figure.

In order to account for the coupling between the flexible boundary and the finite elements it is necessary to determine the stiffness matrix of the half-space corresponding to the DOF along the boundary. It is illuminating at this point to consider the physical meaning of such a stiffness matrix. Due

Department of Civil and Environmental Engineering, Michigan State University, East Lansing, Mich. 48824.

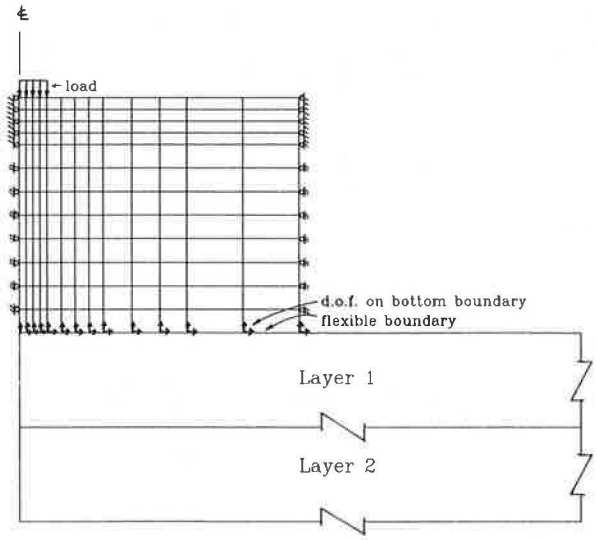

FIGURE 1 Finite-element mesh on flexible boundary.

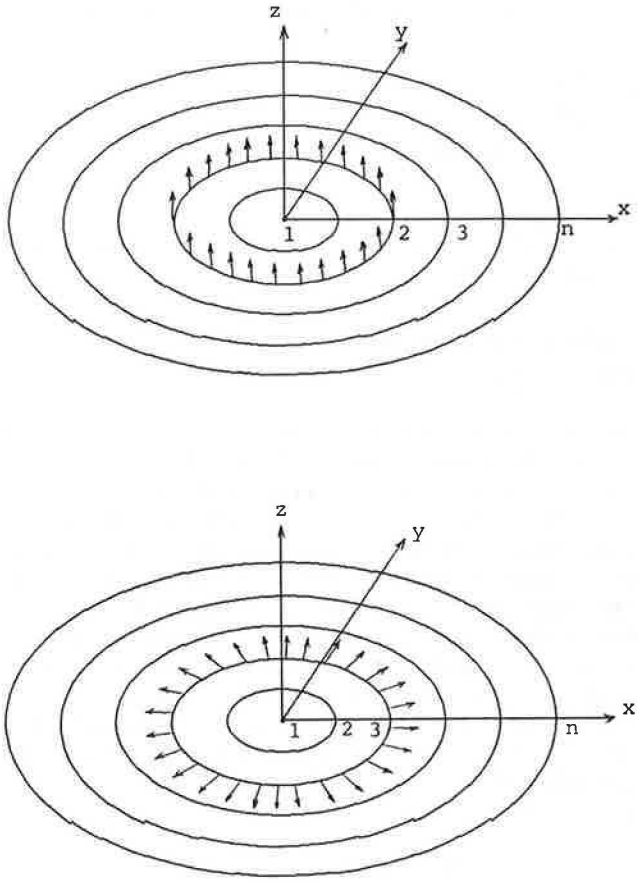

FIGURE 2 Vertical (*top*) and radial (*bottom*) ring loads.

to the axisymmetric nature of the problem, the DOF along the boundary are really the vertical and radial displacements of the rings shown in Figure 2. At the origin the ring degenerates to a point. If there are n rings as shown in the figure, there will be $(2n - 1)$ DOF, since there is no radial DOF at the origin (the radial displacement at the origin is zero due to symmetry). The stiffness matrix will then have dimensions of $[(2n - 1) \times (2n - 1)]$. The element k_{ij} (i row and j column) of the stiffness matrix $\mathbf{K}$ is the total force required along the ring at DOF i when DOF j is displaced by a unit amount while all other DOF are held fixed. The elements of the stiffness matrix are extremely difficult to compute directly. However, the inverse of the stiffness matrix, commonly known as the flexibility matrix, can be computed. The element f_{ij} of the flexibility matrix $\mathbf{F}$ is the displacement along DOF i due to a unit total uniform ring load along DOF j (vertical and radial uniform ring loads are depicted in Figure 2). This displacement can be obtained from an elastic-layer program such as CHEV51. If the boundary is placed within the subgrade, as will be most common, then the half-space will be homogeneous and analytical results can be used to determine the flexibility coefficients.

There is one problem of incompatibility between finite-element modeling and elastic-layer modeling. If finite elements are used to model the half-space beneath the boundary, concentrated ring loads (load per unit arc length) can be applied at the nodes, and all displacements on the boundary can be computed. When the half-space is modeled by elastic-layer theory, however, concentrated ring loads will produce finite displacements at all points on the boundary except directly under the load. On the ring where the load is placed, the displacements will tend to infinity. This, of course, is the true behavior since it is known that plastic deformation will occur under the concentrated load. In order to link together the finite elements and the elastic half-space, however, some approximation is necessary to compute the diagonal elements of the flexibility matrix (these f_{jj} elements are the displacements directly under the ring loads). One possible approximation is to assume that the load is uniformly distributed over the annular surface halfway from the loaded ring to the two adjacent rings. This concept is further discussed below.

Once the flexibility matrix of the half-space has been estimated, it can be inverted to obtain the corresponding stiffness matrix. The DOF along the bottom boundary are usually about 30, and the inversion of a 30×30 symmetric matrix presents no problem. Further, since the half-space below the boundary is assumed to be elastic, this inversion only needs to be performed once even if finite elements are used to model nonlinear materials above the boundary.

The stiffness matrix of the entire system comprising finite elements and the half-space is assembled from the stiffness matrices of each of the subsystems. The stiffness matrices of the finite elements are computed one by one and assembled as usual. This matrix, denoted by $\mathbf{K}_{FE}$, may be partitioned as follows:

$$\mathbf{K}_{FE} = \begin{bmatrix} \mathbf{K}_{FF} & \mathbf{K}_{FB} \\ \mathbf{K}_{BF} & \mathbf{K}_{BB} \end{bmatrix} \tag{1}$$

where the $(2n - 1) \times (2n - 1)$ matrix $\mathbf{K}_{BB}$ corresponds to the DOF along the bottom boundary. The stiffness matrix of the half-space is denoted by $\mathbf{K}_{HS}$, also a $[(2n - 1) \times (2n - 1)]$ matrix). $\mathbf{K}_{BB}$ will have many zero elements (since $\mathbf{K}_{FE}$ is usually a banded matrix), but $\mathbf{K}_{HS}$ will be fully populated. The stiffness matrix of the combined system is then

$$\mathbf{K} = \begin{bmatrix} \mathbf{K}_{FF} & \mathbf{K}_{FB} \\ \mathbf{K}_{BF} & \mathbf{K}_{BB} + \mathbf{K}_{HS} \end{bmatrix} \tag{2}$$

If the nodal displacements **D** are partitioned corresponding to **K** as

$$\mathbf{D} = \begin{bmatrix} \mathbf{D}_F \\ \mathbf{D}_B \end{bmatrix} \tag{3}$$

then the solution of the stiffness equations

$$\mathbf{KD} = \mathbf{Q} \tag{4}$$

will yield the displacements at all nodes, *including those at the boundary*, $\mathbf{D}_B$.

FLEXIBILITIES FOR HOMOGENEOUS HALF-SPACE

As mentioned earlier, in most cases the bottom boundary will be within the subgrade, and the half-space beneath the boundary will be homogeneous. For this case it is possible to use analytical expressions to evaluate the flexibilities of the half-space. Analytical solutions for vertical and radial ring loads may be derived, but in the absence of simple expressions, it is necessary to resort to numerical integration. Elegant closed-form solutions, however, exist for uniform vertical loads and linearly varying radial loads on a circular area. These can be utilized to estimate the required flexibility coefficients.

According to Poulos and Davis (*4*), for a uniform vertical upward load p applied to a circular area of radius r_0 the vertical (upward) and radial (outward) surface displacements are, respectively,

$$w_V(r;r_0;p) = \begin{cases} F(0.5,-0.5;1;(r/r_0)^2)\,\dfrac{2(1-\nu^2)}{E}\,pr_0, & \text{for } r < r_0 \\ \dfrac{4(1-\nu^2)}{\pi E}\,pr_0, & \text{for } r = r_0 \\ F(0.5,0.5;2;(r_0/r)^2)\,\dfrac{(1-\nu^2)}{Er}\,pr_0^2, & \text{for } r > r_0 \end{cases} \tag{5}$$

and

$$u_V(r;r_0;p) = \begin{cases} \dfrac{(1+\nu)(1-2\nu)}{2E}\,pr, & \text{for } r \le r_0 \\ \dfrac{(1+\nu)(1-2\nu)}{2Er}\,pr_0^2, & \text{for } r > r_0 \end{cases} \tag{6}$$

where

r = horizontal distance from center of load;
E, ν = elastic modulus and Poisson's ratio of half-space.

$F(\alpha,\beta;\gamma;x)$ is the hypergeometric function with parameters α, β, and γ, the series representation of which is

$$F(\alpha,\beta;\gamma;x) = 1 + \frac{\alpha,\beta}{(1)\gamma}\,x + \frac{\alpha(\alpha+1)\beta(\beta+1)}{(1)(2)\gamma(\gamma+1)}\,x^2 + \ldots \tag{7}$$

For a radial (outward) load varying linearly from zero at the center to p at distance r_0, acting on a circular area of radius r_0, the vertical and radial displacements are, respectively,

$$w_R(r;r_0;p) = \begin{cases} \dfrac{(1+\nu)(1-2\nu)}{2E}\left(1-\left[\dfrac{r}{r_0}\right]^2\right)pr_0 & \text{for } r < r_0 \\ 0 & \text{for } r \ge r_0 \end{cases} \tag{8}$$

and

$$u_R(r;r_0;p) = \begin{cases} F(1.5,-0.5;2;(r/r_0)^2)\,\dfrac{(1-\nu^2)}{E}\,pr & \text{for } r < r_0 \\ \dfrac{4(1-\nu^2)}{3\pi E}\,pr_0, & \text{for } r = r_0 \\ F(1.5,0.5;3;(r_0/r)^2)\,\dfrac{p(1-\nu^2)}{4E}\left[\dfrac{r_0^3}{r^2}\right] & \text{for } r > r_0 \end{cases} \tag{9}$$

Consider now the two boundary nodes shown in Figure 3, with DOF i and j at node A, and DOF k and l at node B. By approximating the vertical ring load at k by a uniform vertical load over a very thin annulus of width 2ε (see Figure 4), the flexibility coefficients f_{ik}, f_{ji}, and f_{lk} can be estimated as follows:

$$f_{ik} = w_V(r_1;\, r_2 + \varepsilon;\, p_1) - w_V(r_1;\, r_2 - \varepsilon;\, p_1) \tag{10}$$

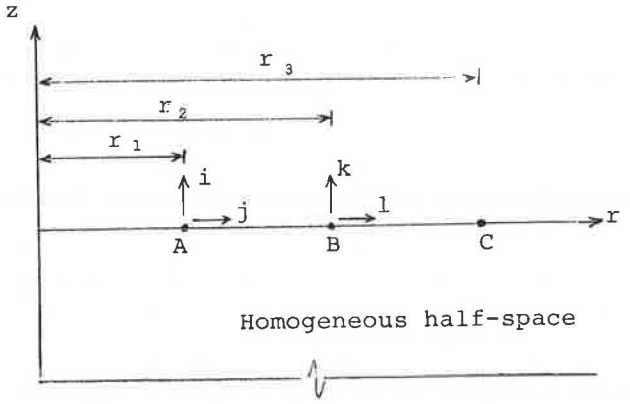

FIGURE 3 Typical nodes and degrees of freedom.

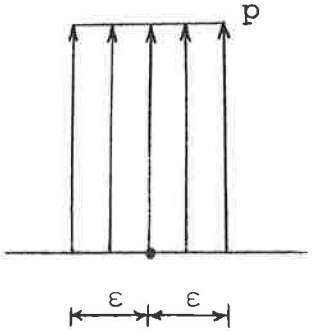

FIGURE 4 Vertical load on thin annulus.

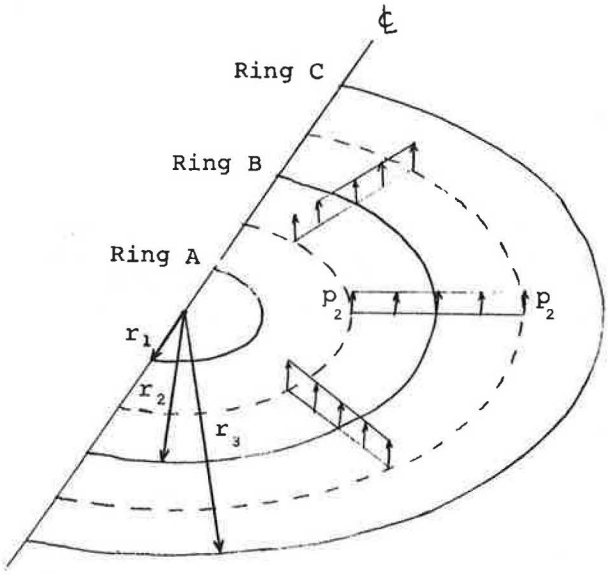

FIGURE 5 Uniform vertical loading to estimate f_{kk}.

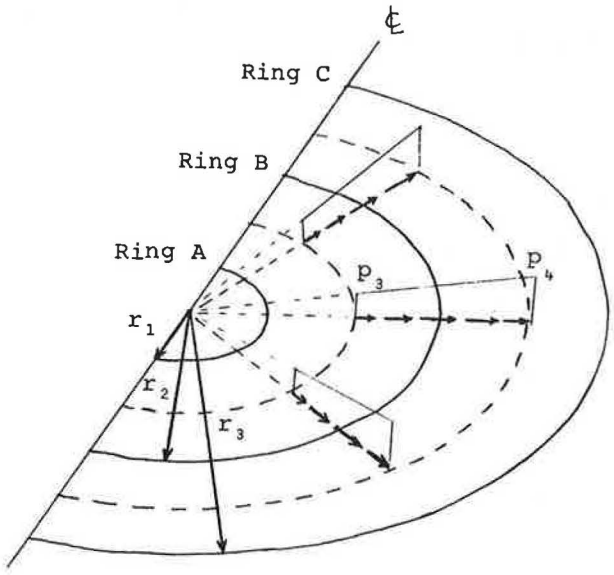

FIGURE 6 Linear radial load to estimate f_{ii}.

$$f_{jk} = u_V(r_1; r_2 + \varepsilon; p_1) - u_V(r_1; r_2 - \varepsilon; p_1) \quad (11)$$

$$f_{lk} = u_V(r_2; r_2 + \varepsilon; p_1) - u_V(r_2; r_2 - \varepsilon; p_1) \quad (12)$$

where

$$p_1 = 1/4\pi\varepsilon r_0 \quad (13)$$

With p_1 defined as in Equation 13, the total load on the annulus is unity. As long as ε is small, these coefficients are not sensitive to the exact magnitude of ε. According to the Maxwell-Betti reciprocal theorem, $f_{ki} = f_{ik}$, $f_{kj} = f_{jk}$, and $f_{kl} = f_{lk}$.

This technique cannot, however, be used to estimate f_{kk} or f_{ll}. These flexibilities are very sensitive to the magnitude of ε. In fact, as mentioned before, as $\varepsilon \to 0$, $f_{kk} \to \infty$ and $f_{ll} \to \infty$. To estimate the diagonal flexibilities, therefore, we assume that a uniform load (with unit total load) is applied in an annulus from midway between nodes A and B to midway between nodes B and C in Figure 3. (For the radial load, a linearly varying load is assumed, again because elegant results exists for this case. The difference in f_{ll} from using a uniform or linear load should be small, and since this is an estimate

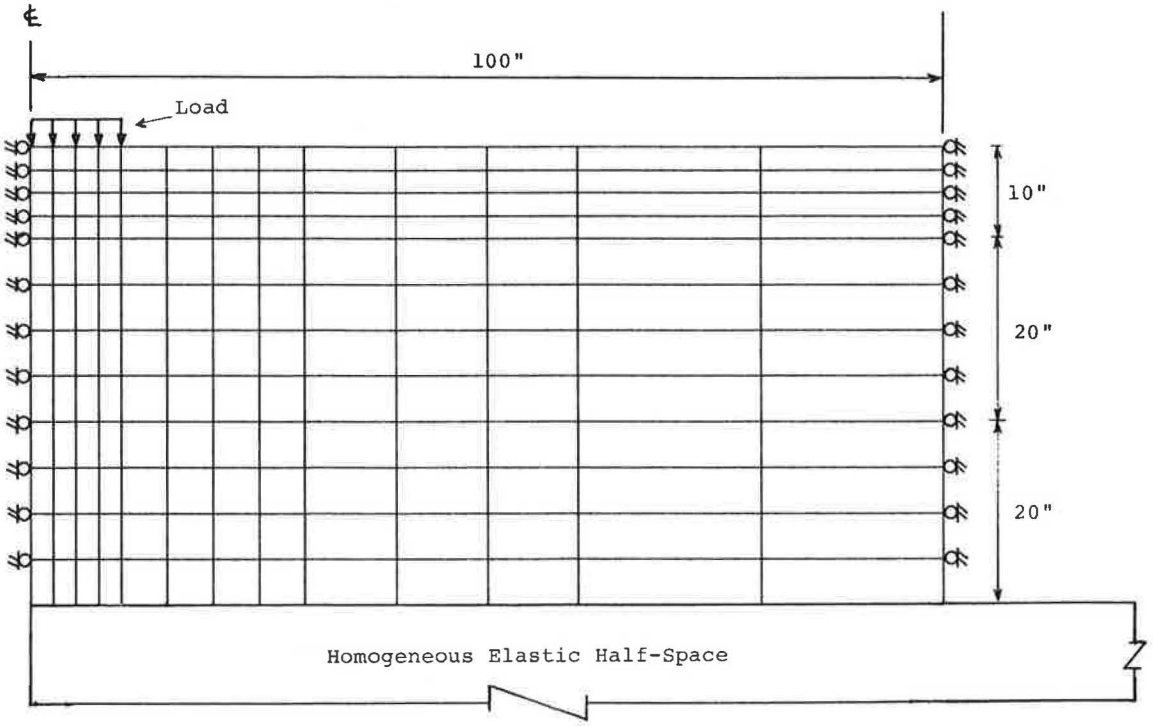

FIGURE 7 Finite-element mesh used with flexible boundary.

anyway, the exact load type is perhaps not too important.) The loading approximations used for the vertical and radial loads are illustrated in Figures 5 and 6. Thus we obtain:

$$f_{kk} \approx w_V(r_2;\ (r_2 + r_3)/2;\ p_2) - w_V(r_2;\ (r_1 + r_2)/2;\ p_2) \tag{14}$$

and

$$f_{ll} \approx u_R(r_2;\ (r_2 + r_3)/2;\ p_4) - u_R(r_2;\ (r_1 + r_2)/2;\ p_3) \tag{15}$$

where

$$p_2 = \frac{1}{\pi[(r_2 + r_3)^2 - (r_1 + r_2)^2)]} \tag{16}$$

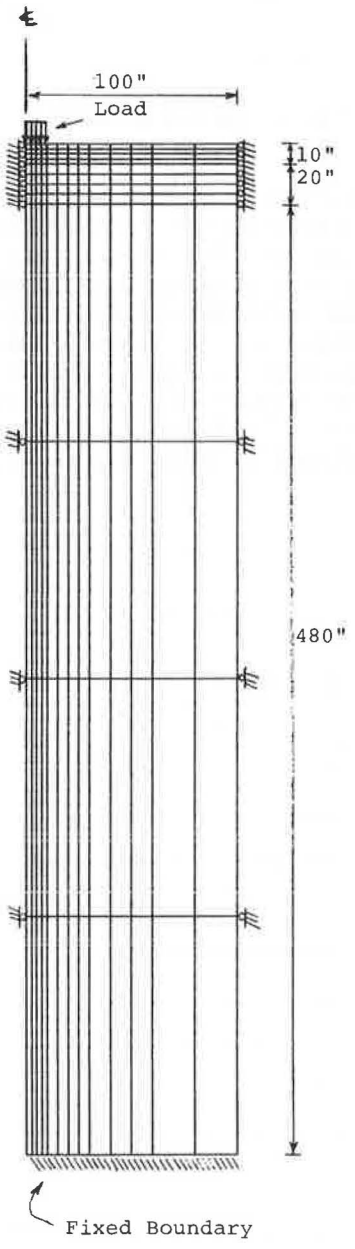

FIGURE 8 Traditional finite-element mesh.

$$p_3 = \frac{6(r_1 + r_2)}{\pi[(r_2 + r_3)^3 - (r_1 + r_2)^3]} \tag{17}$$

and

$$p_4 = p_3 \frac{(r_2 + r_3)}{(r_1 + r_2)} \tag{18}$$

The expressions for p_2, p_3, and p_4 given above ensure the load patterns illustrated in Figures 5 and 6 with the total load in each case being unity. All the diagonal terms of the flexibility matrix can be estimated as in Equations 14 and 15.

NUMERICAL RESULTS FOR HOMOGENEOUS AND MULTILAYERED PAVEMENTS

Analyses using the flexible boundary were performed for homogeneous and multilayered (three-layered) half-spaces. In both cases, a load of 100 psi was applied on a circular area of radius 10 in., and the flexible boundary was placed at a depth of 50 in., above which a finite-element mesh was used. The side boundary was placed at 100 in. from the centerline (10 times the radius of the loaded area) for both cases. The material properties were as follows:

Homogeneous: E = 5,000 psi; ν = 0.45.
Multilayer: Layer 1 (asphalt) – E = 200,000 psi; ν = 0.35; depth = 10 in.;
Layer 2 (base) – E = 15,000 psi; ν = 0.40; depth = 20 in.;
Layer 3 (subgrade) – E = 5,000 psi; ν = 0.45; infinite depth.

In order to compare the results with the traditional finite-element approach, a mesh of depth 510 in. was used with a fixed boundary. [As noted by Duncan et al. (*1*), a deep mesh is required in traditional finite-element analysis.] The number of elements was kept the same in both meshes to facilitate a direct comparison, while keeping the computational effort approximately the same. This meant that in the traditional mesh the deeper elements had very large length-to-width ratios. The mesh used with the flexible boundary and the traditional mesh (finite elements only) are shown in Figures 7 and 8, respectively. The same meshes were used for the homogeneous and multilayered cases.

The vertical displacements along the top free surface and the variation of the vertical displacement with depth beneath the center of the loaded area are shown in Figures 9 and 10. The percentage errors in both finite-element approaches, as compared with the exact results, are tabulated in Tables 1 and 2. (The abbreviations "FE + FB" and "FE only" are used to denote "finite elements plus flexible boundary" and "finite elements only," respectively, in the figures and tables.) It is apparent that use of the flexible boundary gives much better results, especially for the multilayered case where displacements within the subgrade contribute significantly toward the total displacements. The flexible boundary approach is more accurate for the homogeneous case than for the multilayered case, but in both cases it is more accurate than the traditional finite-element approach.

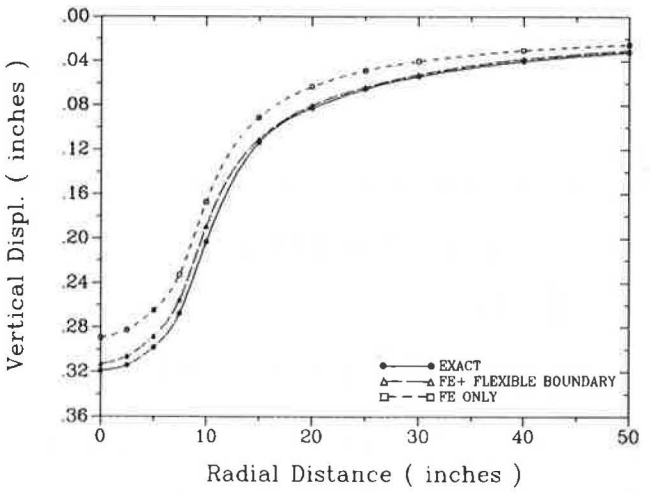

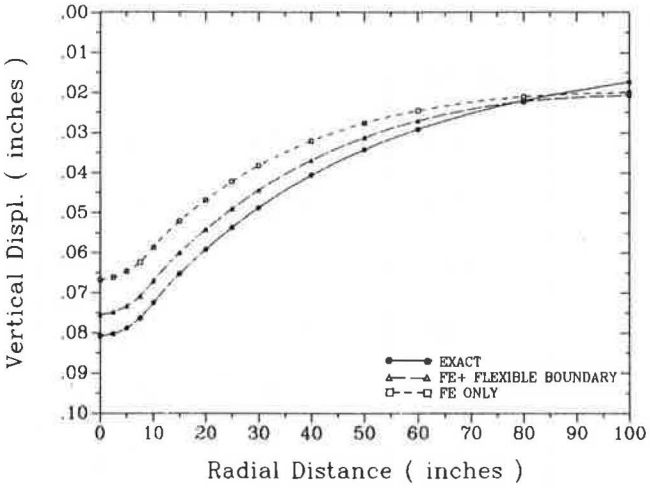

FIGURE 9 Vertical surface displacement: homogeneous (*top*); multilayer (*bottom*).

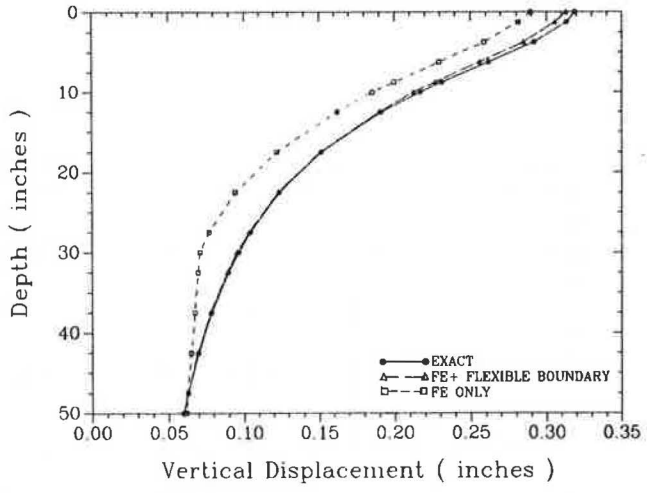

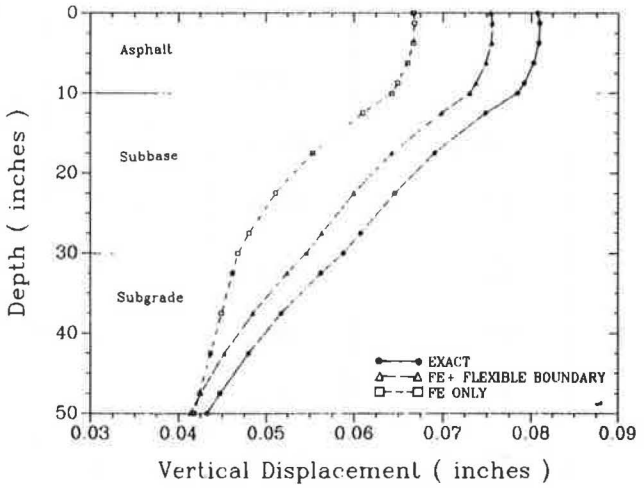

FIGURE 10 Vertical displacement beneath center of load: homogeneous (*top*); multilayer (*bottom*).

The variation of vertical and radial stresses with depth beneath the center of the loaded area is presented in Figures 11 and 12, respectively. The percentage errors, as compared with exact results, are tabulated in Tables 3 and 4. Again, use of the flexible boundary gives better results than the traditional approach. The differences in the stresses, however, are less significant than those in the displacements. For the homogeneous case, at depths below 30 in., the actual radial stresses are very small. Because of this, a comparison of the percentage errors (which were very large) is somewhat meaningless and has been omitted from Table 4. For the same reason, the percentage errors are very large for the traditional approach at large depths. The percentage errors should be compared with the value of the actual stresses in mind.

One point worth noting is the lack of accuracy of the finite-element method (both with and without the flexible boundary) when stresses are evaluated near the corners of elements (i.e., near nodes). Stresses are most accurate at the middle of the elements and are reasonable at the middle of element edges, but not accurate near element corners. For homogeneous material the stresses from finite-element solutions are not continuous across element boundaries (as they should be). This is the reason for the large errors in the radial stresses at depths of 10 in. and 30 in. (see Table 4). These depths represent the interfaces between layers for the multilayered case. Also, when elements with very large aspect ratios [such as the deeper elements in the traditional mesh (Fig. 8)] are used, the results tend to be poor. A better mesh than the one in Figure 8 would require many more elements and hence would result in a much greater computational effort.

A number of case studies were performed using the flexible boundary approach, varying the moduli and thicknesses of the base and subbase layers. In all cases the results compared favorably with the exact solutions.

TABLE 1 ERRORS IN VERTICAL SURFACE DISPLACEMENTS

	Homogeneous			Multilayer		
Radial Dist. (inches)	Exact Displ. (inch)	Percentage Error		Exact Displ. (inch)	Percentage Error	
		FE + FB	FE only		FE + FB	FE only
0	.3190	-1.9	-9.3	.0807	-6.6	-17.4
2.5	.3140	-2.6	-10.1	.0802	-6.8	-17.6
5	.2980	-3.3	-11.1	.0788	-6.9	-17.9
7.5	.2677	-4.6	-13.1	.0763	-7.1	-18.3
10	.2031	-6.8	-17.7	.0725	-7.5	-19.0
15	.1136	-2.5	-19.8	.0653	-8.0	-20.2
20	.0825	-2.8	-23.6	.0592	-8.4	-20.9
25	.0652	-2.5	-25.4	.0537	-8.7	-21.4
30	.0539	-3.0	-25.1	.0488	-8.9	-21.5
40	.0401	-4.6	-24.4	.0406	-9.1	-21.0
50	.0321	-5.6	-21.9	.0342	-8.9	-19.4
60	.0266	-4.7	-17.8	.0292	-7.3	-16.0
80	.0201	-4.8	-12.0	.0220	0.9	-4.6
100	.0160	6.4	3.1	.0173	19.3	15.2

TABLE 2 ERRORS IN VERTICAL DISPLACEMENTS BENEATH CENTER OF LOAD

	Homogeneous			Multilayer		
Vert. Dist. (inches)	Exact Displ. (inch)	Percentage Error		Exact Displ. (inch)	Percentage Error	
		FE + FB	FE only		FE + FB	FE only
0	.3190	-1.9	-9.3	.0807	-6.6	-17.4
1.25	.3134	-2.5	-10.3	.0810	-6.7	-17.5
3.75	.2916	-2.4	-11.1	.0809	-6.6	-17.5
6.25	.2620	-2.3	-12.3	.0803	-6.7	-17.7
8.75	.2314	-1.9	-13.6	.0792	-6.8	-18.0
10	.2171	-2.0	-14.5	.0784	-6.8	-17.2
12.5	.1913	-0.6	-15.2	.0749	-6.7	-18.5
17.5	.1516	-0.4	-19.4	.0691	-7.0	-19.9
22.5	.1239	-0.6	-23.9	.0646	-7.1	-20.9
27.5	.1042	-0.8	-26.1	.0608	-7.2	-20.9
30	.0964	-1.4	-26.4	.0588	-7.1	-20.5
32.5	.0897	-0.9	-22.2	.0563	-6.8	-18.0
37.5	.0785	-0.6	-14.1	.0518	-6.3	-13.3
42.5	.0698	-0.4	-6.7	.0480	-5.8	-9.1
47.5	.0628	-0.0	-0.0	.0447	-4.9	-5.2
50	.0598	-0.0	+2.7	.0433	-4.5	-3.4

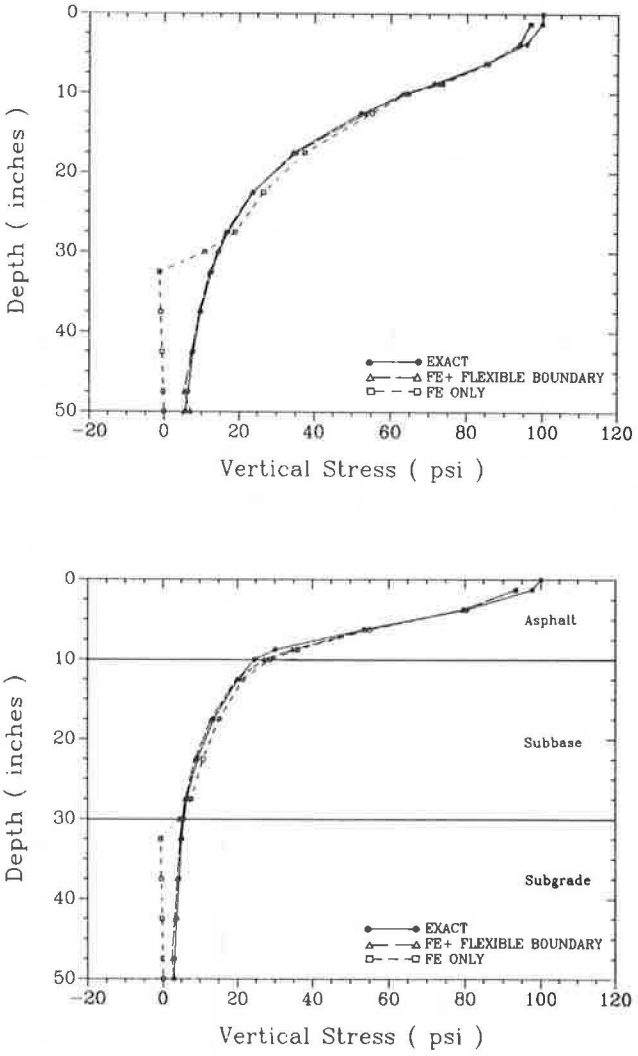

FIGURE 11 Vertical stress beneath center of load: homogeneous (*top*); multilayer (*bottom*).

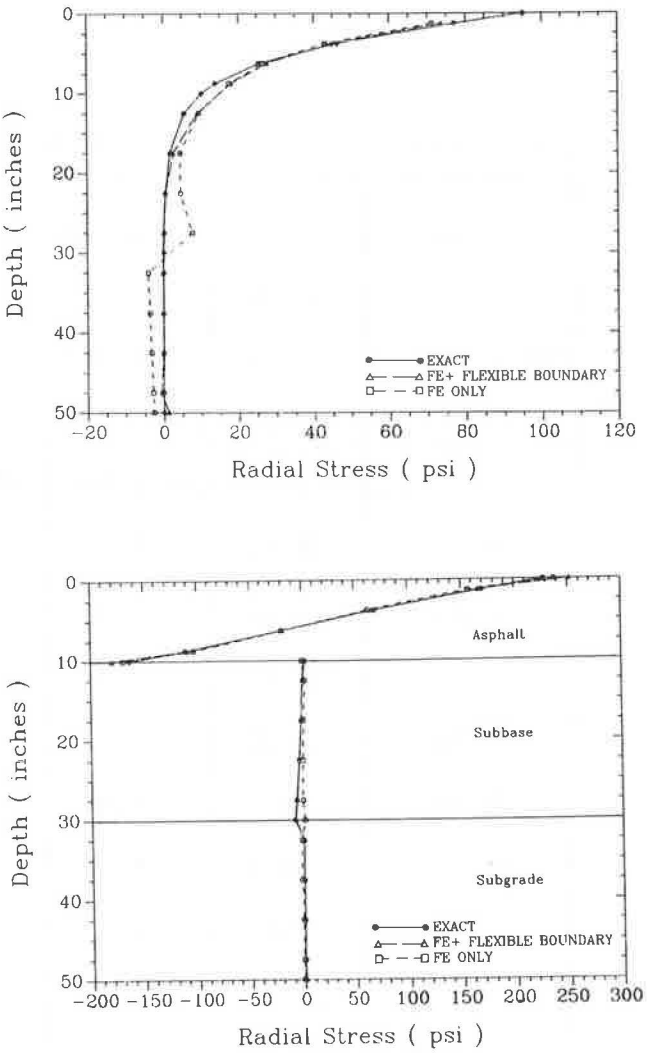

FIGURE 12 Radial stress beneath center of load: homogeneous (*top*); multilayer (*bottom*).

CONCLUSIONS

A new technique is developed to model the flexibility of the bottom boundary used in static finite-element analyses of pavements. Such modeling enables the bottom boundary to be placed at any depth below which displacements and stresses are not of interest, while accurately representing the displacements occurring in the material below the boundary. Results indicate that the method is accurate. The principal advantage of this new technique is its computational efficiency, especially when used with nonlinear finite-element approaches requiring iterative or incremental solutions. The use of a flexible boundary also yields significantly better results than a traditional finite-element approach requiring approximately the same amount of computational effort.

ACKNOWLEDGMENT

The work described in this paper was sponsored by the Michigan Department of Transportation. It represents part of the efforts devoted to developing a nonlinear finite-element program for the analysis of flexible pavements.

TABLE 3 ERRORS IN VERTICAL STRESSES BENEATH CENTER OF LOAD

	Homogeneous			Multilayer		
Vert. Dist. (inches)	Exact Stress (psi)	Percentage Error		Exact Stress (psi)	Percentage Error	
		FE + FB	FE only		FE + FB	FE only
1.25	99.81	-3.2	-3.0	97.62	-4.5	-4.4
3.75	95.67	-2.0	-1.8	80.43	-1.3	-0.7
6.25	85.11	-0.0	0.6	53.54	1.1	2.7
8.75	71.45	1.8	2.9	30.11	15.3	19.7
10	64.64	-2.3	-0.5	24.62	10.7	16.9
12.5	52.39	2.3	5.2	20.26	-2.3	6.3
17.5	34.55	1.7	8.6	13.68	-4.6	10.7
22.5	23.69	-0.6	11.8	9.25	-6.2	16.8
27.5	17.00	-2.7	11.7	6.44	-6.8	17.9
30	14.62	-1.6	-25.5	5.65	-6.1	-18.2
32.5	12.69	-3.7	-110.	5.13	-10.3	-112.
37.5	9.79	-3.9	-109.	4.30	-11.3	-109.
42.5	7.76	-4.6	-107.	3.66	-13.0	-106.
47.5	6.30	-14.9	-103.	3.15	-23.6	-100.
50	5.71	22.8	-101.	2.94	1.1	-97.

TABLE 4 ERRORS IN RADIAL STRESSES BENEATH CENTER OF LOAD

	Homogeneous			Multilayer		
Vert. Dist. (inches)	Exact Stress (psi)	Percentage Error		Exact Stress (psi)	Percentage Error	
		FE + FB	FE only		FE + FB	FE only
1.25	77.11	-4.5	-7.6	169.9	-2.2	-7.8
3.75	46.25	-3.3	-7.0	69.39	-3.7	-9.7
6.25	25.59	7.9	3.6	-19.36	3.0	-1.7
8.75	13.79	31.1	27.5	-111.0	-1.8	-7.3
10 (+)	10.15	159.	158.	-163.5	9.9	3.7
10 (-)	10.15	176.	181.	2.05	-217.	-128.
12.5	5.58	62.2	68.8	.54	25.7	352.
17.5	1.83	46.4	145.	-1.63	-9.3	150.
22.5	.65	-9.7	602.	-3.66	-8.9	103.
27.5	.23	-95.3	3197.	-6.27	-9.0	-97.2
30 (+)	.13	-	-	-8.04	-8.6	121.
30 (-)	.13	-	-	3.28	-131.	-165.
32.5	.07	-	-	.28	6.4	-821.
37.5	.00	-	-	.22	25.1	-949.
42.5	-.03	-	-	.17	44.6	-1064.
47.5	-.04	-	-	.14	-106.	-1131.
50	-.04	-	-	.12	403.	-1149.

REFERENCES

1. J. M. Duncan, C. L. Monismith, and E. L. Wilson. Finite Element Analysis of Pavements. In *Highway Research Record 228,* HRB, National Research Council, Washington, D.C., 1968, pp. 18–33.
2. S. F. Brown and J. W. Pappin. Analysis of Pavements with Granular Bases. In *Transportation Research Record 810,* TRB, National Research Council, Washington, D.C., 1981, pp. 17–23.
3. L. Raad and J. L. Figueroa. Load Response of Transportation Support Systems. *Transportation Engineering Journal, ASCE,* Vol. 106, No. TE1, 1980, pp. 111–128.
4. H. G. Poulos and E. H. Davis. *Elastic Solutions for Soil and Rock Mechanics,* Wiley, New York, 1974.

Publication of this paper sponsored by Committee on Flexible Pavement Design.